Design of an Energy Storage System for the Tokamak ISTTOK

Pedro Miguel de Castro Pena Brandão Rodrigues
Instituto Superior Técnico
pedro.brandao.rodrigues@tecnico.ulisboa.pt

***Abstract*—This paper addresses the design of an energy storage system (ESS) for the research fusion device ISTTOK. The purpose of this work is to study, simulate and design a supplement for this tokamak, which has an operation cycle characterized by a pulse of 3 s and a rest period of approximately 15 min. The system is designed to supply the coils that produce the toroidal magnetic field, used for plasma confinement, but also to retrieve most of the energy stored in these coils during the operation. The solutions developed are compared, lastly, the feasibility of each is accessed. The data and features of the tokamak ISTTOK are presented, with special emphasis on the toroidal field (TF) system. The existing 1 MVA thyristor based power supply is studied and simulated. New energy recovery resonant converter topologies are proposed, to be able to cope with currents near 10 kA. The most appropriate energy storage technologies are discussed and compared based on their characteristics.**

***Index Terms*—Tokamak, Energy Storage, Power supply, Supercapacitors, Toroidal Field.**

I. Introduction

The application of nuclear fusion energy for power generation is becoming more prevalent as a subject of study and experiment. Nuclear fusion has great potential due to the large amount of energy released on nuclear reactions, however, the process of transforming this energy into electrical energy is extremely challenging and complex. The technology and knowledge to assemble sustainable nuclear fusion power plants are still lacking, and the viability of this process is being assessed [1].

Currently, tokamaks are the main candidates for nuclear fusion reactors. Tokamak reactors are devices capable of confining hot plasmas through strong magnetic fields in the shape of a torus, thus creating conditions for thermonuclear fusion to be possible. The operation is based on the interaction between magnetic fields and plasma. This state of matter is electrically conductive, therefore can be manipulated with electric and magnetic fields [2]. Generally, tokamaks are composed of three main electromagnetic systems: ohmic heating system, equilibrium field system, and TF system [3].

The ISTTOK is a relatively small tokamak at IST (Instituto Superior Técnico), with a circular cross-section and an iron core transformer [4]. The TF system requires high current for the coils, as a result, the leftover energy stored on this inductor is significant. Unfortunately, this remaining energy is not reused in the tokamak, instead, it is injected back into the public grid, causing minor disturbances and power quality issues. Consequently, EDP charges this re-injected energy as reactive energy. The solution for this problem is to store, after the operation, the remaining energy into an ESS.

The ISTTOK is a pulse power application that works in an intermittent regime. The operation is characterized by a cycle with a pulse duration of 3 seconds and a rest period (interval between pulses) of approximately 15 minutes. The TF System includes the coils that produce the toroidal magnetic field, and their power supply which will be analysed in detail in section III. This magnetic field has the maximum reach of 2.8 T, this value corresponds to a current intensity of 40 kA. However, due to the power restriction of 1 MVA imposed by the public grid, the toroidal magnetic field density is limited to approximately 0.5 T, which corresponds to a current intensity of 8500 A. The minimum value for the MF that is enough for the project is 0.3 T, this corresponds to a current intensity of 4000 A [5]. The TF is produced by a toroidal solenoid made of 24 coils with water cooling. The data for these coils is presented in Table I.

TABLE I
Parameters of the TF coils of the ISTTOK, adapted from [5].

Toroidal Solenoid Parameters	Value
Number of coils	24
Maximum current	40 kA
Maximum magnetic field	2.8 T
Electrical resistance	10 mΩ
Inductance	1.88 mH
Time constant	0.188 s

II. Energy Storage Technologies

Energy storage technologies (EST) are acknowledged as an essential element in the modern energy supply chain [6]. ESSs are capable of storing the excess energy generated so it can be later converted into useful energy. Some of the main applications are the adjustment of fluctuations in renewable energy sources, making them more reliable for steady energy supply, the improvement of efficiency and the enhancement of grid stability [7].

In order to evaluate if a given EST is suitable for a specific energy storage application there are some factors that must be taken into account. There are specific features that help determine what are the possible applications of a certain technology. The most important characteristics are: energy density, power density, storage capacity, storage duration, life time, round trip efficiency, response time, costs and technological maturity [6], [8]. Table II shows a few ESTs and their technical features.

Considering the parameters and the technical characteristics presented in Table II, four candidates were selected for this specific application (ISTTOK): flywheels, high power density

TABLE II
TECHNICAL CHARACTERISTICS OF ESTS, ADAPTED FROM [6]–[9].

Technology	Specific energy (Wh/kg)	Energy density (kWh/m^3)	Specific power (Wh/kg)	Power density (kWh/m^3)	Power Rating
Flywheel	10-100	20-400	400-1500	1000-5000	0-250 kW
Supercapacitor	2.5-15	10-30	500-5000	10,000- >50,000	0-300 kW
Capacitor	<0.5	0.1-5	10000-50000	>100000	0-400 kW
Li-ion battery	60-200	200-750	500-2000	1500-10,000	0-100 kW
NaS battery	100-240	150-300	150-230	120-230	50 kW-8 MW
SMES	0.5-5	0.2-2.5	500-2000	1000-4000	100 kW-10 MW

Technology	Discharge time	Suitable storage duration	Life time (years)	Cycle life	Round trip efficiency (%)
Flywheel	ms - 15 min	s - min	~15	>20,000	85-95
Supercapacitor	ms - 60 min	s -h	>15	>100,000	90-95
Capacitor	us - s	ms -min	~5	<50000	70-90
Li-ion battery	min - h	min - days	10	1000-10,000	85-95
NaS battery	s - h	s -h	10 - 15	2500	70-90
SMES	ms - 10 s	min - h	>20	>100,000	90-98

batteries, supercapacitors and regular capacitors. Each of these ESSs was analysed taking into consideration the principle of operation, the main characteristics, the advantages and disadvantages, and the common applications. Lastly, it was evaluated if the application of the EST was suitable for the ESS of the ISTTOK.

Starting with the Flywheels, they store energy in mechanical form, more specifically kinetic energy [10]. The coils that create the TF operate with high currents and relatively low voltages [5]. As a consequence, the generator that converts the kinetic energy of the flywheel into electrical energy would have to withstand this intensity of the current. Generators with this capacity have large dimensions and are very expensive, thus not suitable in this case. Also, flywheel units have the capability to produce higher voltages, therefore, the installation of transformers is generally required [11]. The operation conditions of the ISTTOK implies a 15 min rest period. This is a long duration for a flywheel without vacuum chamber and magnetic levitation to store energy without too many losses. Taking into consideration all the factors discussed, the application of a FESS to this case would be very expensive and not adequate.

Battery energy storage is classified as electrochemical energy storage and is regarded as the most developed and used [9]. There are many types of batteries but currently, lithium cells have gained a major role in ESSs, due to the numerous advantages over other types. Among the lithium battery types, Li-ion is the most prominent [12] and are the main candidates for power applications. The tokamak operation is characterized by high-power pulses. Batteries are not the most appropriate technology for this purpose due to the low power density when compared to other ESTs. On the other hand, the energy density is excessive, therefore, a lot of the storage capacity would be wasted. The number of cycles and life span is also a drawback. Considering these factors, the application of batteries is not adequate.

Supercapacitor energy storage is classified as electrochemical energy storage. In comparison to conventional capacitors, the storage capacity is much higher, however, supercapacitor cells have low voltage levels [6]. The tokamak operates with high currents and relatively low voltages, these conditions validate the application of supercapacitors. This EST is capable of high power output in short periods of time which is appropriate for pulsed applications like the tokamak. The major issue is the short amount of energy that supercapacitors are able to store when compared with the other storage technologies, nevertheless the energy requirement for this application is not excessive. Another pertinent concern is the discharge curve of the capacitors, which is not flat. This means that the voltage does not remain constant as the energy is used up. Considering all of the factors presented, this candidate appears to be the most promising.

Electrolytic capacitors store the electric energy statically. In comparison to supercapacitors the capacitance is much smaller, however, electrolytic capacitors are capable of charging and discharging in milliseconds [13]. Of all the storage technologies presented in this chapter this one has the highest power density and lowest energy density. Due to the very low energy density of these capacitors the only possible application on the TF system is to store the energy left in the coils at the end of the pulse. Since this type of cells are able to charge and discharge very quickly, the energy transfer between the coils and the electrolytic capacitors can be very fast, insuring few losses during this process.

III. EXISTING POWER SUPPLY

The coils that produce the toroidal MF of the ISTTOK are supplied by a DC power supply. This one megawatt power supply is a 12-pulse assembly based on the parallel association of 4 three-phase thyristors half-wave rectifiers. The power supply is composed by 3 main blocks: measuring and protection equipment, step-down transformers and rectifier with controllable output current [5].

A. Step-Down Power transformers

The rectifier power supply is connected to the Medium Voltage (10 kV) grid, of EDP. Before the rectification stage, the voltage must be reduced, which is performed by two power transformers. Both transformers have a three-phase double star secondary connection, with opposite phase windings (180 degrees out of phase). For the primary side, one of the transformers is connected in star configuration and the other in delta configuration. As a result, a 30 degrees phase shift is

achieved between the secondary voltages of the two power transformers [5]. With this configuration, it is obtained a twelve-pulse system.

B. Twelve-Pulse Rectifier

When the AC sources of the rectifiers are out of phase the connection must be performed via an interphase reactor (transformer). The input terminals of this transformer are connected to the output of each rectifier, and the common point in the middle of the windings, output terminal, is connected to the next stage or the load. The implementation of the rectifier is represented in Figure 1. The system can be divided into two six-phase associations, the left connected to the YYY transformer (star configuration) and the right connected to the DYY transformer (delta configuration).

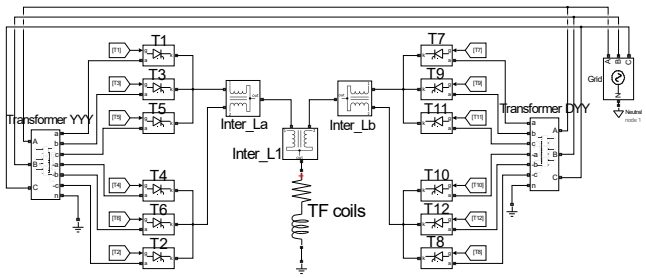

Fig. 1. Simulink implementation of the power section of the rectifier circuit.

The output voltage is characterized by a pulse index of 12 [5]. Its average value is given by

$$U_{0av} = V_M \frac{3}{\pi} \sin\frac{\pi}{3} \cos\epsilon \tag{1}$$

Where U_{0av} is the average value of the output voltage, V_M is the amplitude of the electromotive forces induced on the secondary windings of the power transformers, and ϵ the trigger angle of the thyristors. It is also important to refer that the average value of the output voltage of the three-phase, six-phase and twelve-phase systems is the same. In order to obtain the amplitude of the output voltage, it is possible to consider the parallel association of 4 three-phase half-wave rectifiers equivalent to a twelve-phase half-wave rectifier [5]. As a result, it is established that

$$U_{0M} = V_M \cos\frac{\pi}{6} \cos\frac{\pi}{12} \tag{2}$$

Where U_{0M} is the amplitude of the output voltage. It is essential to analyse the voltage waveforms in different points of the circuit. The simulation of the steady-state voltage at the output of 5 crucial stages of the rectifier is represented in Figure 2, for a trigger angle of 45 degrees. The signals u1 and u2 are the output voltages of the first three-phase rectifier (T1, T3 and T5), and the second three-phase rectifier (T4, T6 and T2), respectively. The signals uY and uD are the output voltages of the two six-phase systems, and Uo is the output voltage of the whole system.

C. Proportional Integral (PI) Controllers

The control of the output current is achieved with PI control. The TF coils are an extremely inductive load with little resistance, consequently, it is expected a pole at the origin. This factor establishes the control model to be adapted which is represented in Figure 3. Each block corresponds to the transfer function of a component. The blue block is the PI compensator, the green block is the rectifier, and the yellow block the inductive load (TF coils). The values of the parameters were obtained based on the content presented in the literature [14].

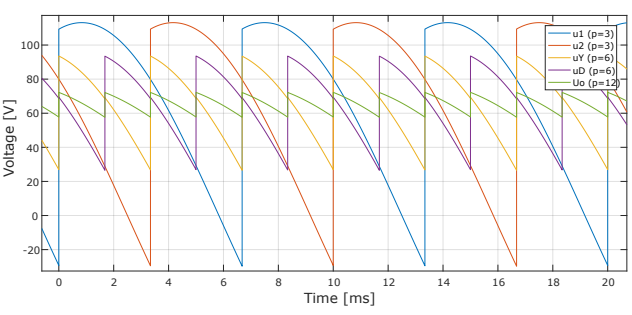

Fig. 2. Steady-state voltages at different points of the rectifier for a 45° trigger angle. Waveforms and corresponding pulse index (p).

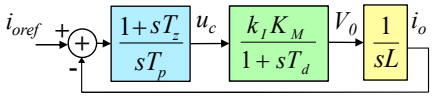

Fig. 3. Control model for the output current and transfer functions.

Due to the parallel association of 4 three-phase rectifiers, the current should be equally divided by the four paralleled fractions. The control of the output current is achieved with feedback loops in each of the 4 three-phase systems. The trigger angle for each group of three thyristors is adjusted based on the current measured at the output of each of these systems.

D. Results of the Current Control

The PI compensator is not able to enforce the control objective instantaneously. The time evolution of the output current is shown in Figure 4, for a desired current of 6000 A. It is possible to compare the results obtained from simulation 4 (a) with the experimental results of the real system 4 (b).

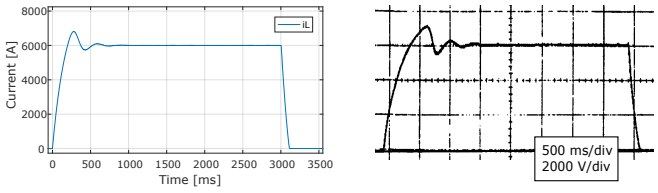

Fig. 4. Evolution of the output current for a reference of 6 kA: (a) Simulink simulation; (b) real system, adapted from [5]. Initial transient response

Figure 4 also shows the cancellation of the current flowing through the coils. It takes a few milliseconds for the current value to reach zero, during this period the energy left in the coils is re-injected into the grid. This behavior can be confirmed by analysing the voltage across the TF coils at the end of the pulse. Figure 5 shows a negative voltage at the terminals of the coils during the cancellation of the current.

Since the current is positive and the voltage negative, it means that the TF coils are supplying energy to the AC network.

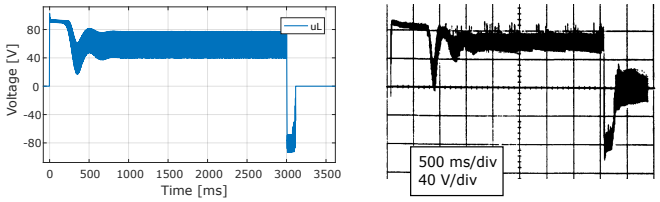

Fig. 5. Evolution of the output voltage for a reference of 6 kA: (a) Simulink simulation; (b) real system, adapted from [5]. And voltage polarity reversal.

IV. Design of an Energy Storage System for the ISTTOK

This section covers the different options that were developed and analysed for the ESS. Although they serve similar purposes each alternative has its own functionality and advantages. There are 3 main solutions which are presented in separate sections of this chapter: supercapacitor power supply with additional DC source, modified rectifier power supply with auxiliary capacitor banks, and energy recover upgrade of the existing power supply. The idea and concepts of each solution is explained, along with the computations and the results including the simulation of the circuits.

Firstly there are a few initial considerations that it is important to keep in mind. Starting with the power dissipation in the coils during the pulse this is the power requirement for the source. This value is obtained with Joule's law. The energy dissipated in the coils is the energy that the power supply needs to provide. This value is obtain by multiplying the power dissipation by the operation time. The magnetic energy left in the TF coils is computed using the inductance of the coils, and the equation for the energy stored in an inductor.

A. Supercapacitor Power Supply with Additional DC Source (1st Solution)

The possibility of replacing the existent power supply with a supercapacitor based power supply is assessed. This solution has the potential to increase the current pulse duration and intensity, to obtain better current rise and fall times, and to recover part of the magnetic energy. The capacitor bank (CB) is charged during the interval between pulses and discharged during the pulse which only lasts a few seconds. The energy stored in the CB must be enough to withstand a current pulse with a specific current intensity and duration. In this solution, the storage system may use another power supply to charge the CB. This DC source can be much smaller and does not need to provide high current, since its function is to only charge the supercapacitors during the period between pulses, which takes a few minutes. By replacing the existing rectifier power supply with a smaller source, which is exclusively responsible for restoring the voltage on the supercapacitor bank, it is possible to reduce the contracted power tariff.

It is crucial to size an optimized CB by minimizing the number of cells needed. The CB is formed by associating capacitor cells (CCs) in series and parallel, thus many combinations are possible. The best association is determined by 3 factors: desired current intensity, duration of the pulse, and the selected CCs. It is important to note that the configuration that minimizes the number of cells, calculated based on these factors, is only optimal for the particular situation used to determine it. The first step to size the supercapacitor bank is to compute the minimum and maximum operating voltage which maximizes the useful energy and meets the power demand. The optimal maximum voltage must be determined using an iterative method, and by selecting the solution that leads to less CCs. The number of CCs in series (Ns) is easy to compute, however the number of CCs that are required in parallel (Np) is given by the following nonlinear equation

$$Np = 2\frac{I_p^2 t_p (R_L + \frac{ESR_c Ns}{Np})}{V_{max}^2 - (I_p(R_L + \frac{ESR_c Ns}{Np}))^2}\frac{Ns}{C_c} \tag{3}$$

Where I_p desired pulse current, R_L the resistance of the coils, t_p the pulse duration, ESR_c the equivalent series resistance (ESR) of the CCs, V_{max} the maximum voltage of the supercapacitor bank, and C_c the capacitance of each cell.

The connection between the CB and the TF coils is carried out using a power converter capable of charging the TF coils and recovering the remaining energy. This implies that the circuit must operate in the first and fourth quadrant, characterised by positive current and both positive and negative voltage. As a result, the converter was inspired in the two-quadrant voltage reversible chopper, modified so that the recovered energy is only delivered to one of the two storage capacitors. The implementation of this circuit is represented in Figure 6. The capacitor C2 represents the supercapacitor bank, and the capacitor C1 represents an electrolytic capacitor bank (ECB). The purpose of adding an ECB is to obtain better current rise and fall times, and to recover more energy. The circuit can be divided in two parts, the power part Figure 6 (a) and the control part Figure 6 (b). The control circuit (low power) is responsible for providing the control signals to the semiconductor switches (S1 and S2), which are IGBTs. Rc1 and Rc2 are the ESRs of the CBs. The DC source used to charge the supercapacitor bank is represented by the voltage source Vs and the internal resistor Rs.

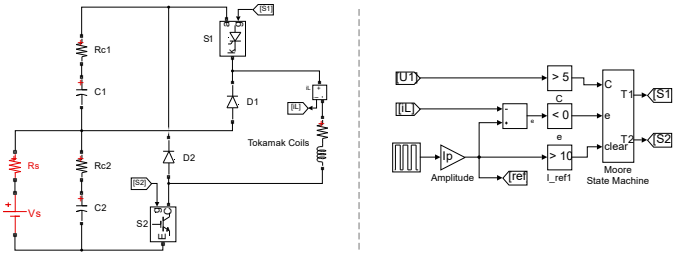

Fig. 6. [Circuit 1.2] Supercapacitor power supply with an electrolytic capacitor bank: (a) power part; (b) control part.

Now it will be presented the main results obtained for a pulse of 8500 A with 3 s. Starting with the current flowing through the TF coils, Figure 7 represents the reference (Iref) and the actual current measured (IL). It takes approximately 23 ms for the current to rise to 8500 A and 28 ms for the current to drop to 0 A, this is considerably faster than a circuit without the ECB. Figure 7 (b) shows the voltage across the coils during the pulse. The initial voltage applied to the coils corresponds to the sum of the voltages at the terminals of the supercapacitor bank (C2) and the ECB (C1). The ECB

was sized to withstand 800 V (nominal voltage), therefore, the initial voltage across the coils is very high (980.9 V) which is why the rise time of the current was shortened so much in relation to Figure 4. The higher the voltage applied to the coils the less time it takes to energize them. At the end of the pulse the polarity of the voltage is inverted reaching -782.2 V. In this case, the energy that is returned to the CB is approximately 57 kJ and corresponds to about 84 % of the magnetic energy left in the TF coils at the end of the pulse.

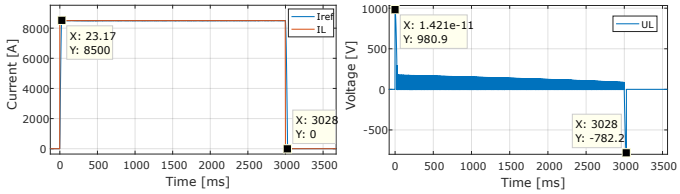

Fig. 7. Simulation results for a pulse of 8500 A with 3 s: (a) current through the TF coils; (b)voltage across the coils. Reduced current rise and fall times.

B. Modified Rectifier Power Supply with Auxiliary Capacitor Banks (2nd Solution)

The possibility of modifying the configuration of the rectifier power supply and integrating a supercapacitor bank is assessed. The purpose of this solution is to increase the maximum current intensity of the pulse, using the existing power supply slightly modified. In order to achieve higher current pulses the output voltage of the power supply must be higher, as a result, the present rectifier configuration (parallel association of 4 three-phase rectifiers) must be modified. These three-phase rectifiers must be connected in series which results in an output voltage approximately 4 times higher than the standard configuration. However, the maximum current intensity will decrease 4 times, since the power limit has to be equivalent. Consequently, it is not enough to only change the power supply, this is why the integration of a supercapacitor bank is required. The CB must be sized in conjunction with the power supply to withstand the desired current intensity of the pulse. During the period between pulses the bank is charged using the same power supply. This solution is identical to the first one, but now the DC source that was only used to charge the CB between the pulses, is replaced with the existing rectifier which also operates during the pulse, reducing the power and energy demand on the supercapacitor bank.

The sizing process of the CB is similar to the one used for the first solution, however in this case, there is a power supply in parallel with the supercapacitor bank which also supplies the coils during the pulse. As a result, the CB does not need to be as big as before to provide the energy and power demand. Just like before, the CB is optimized for a specific combination of parameters: desired current intensity, duration of the pulse and the selected supercapacitor cell. Together, the CB and the power supply must be able to sustain the desired current of the pulse during the defined time interval, this is only possible if the voltage of the supercapacitor bank is kept above a certain level (minimum voltage) during the pulse. The maximum voltage of the CB is determined by the maximum voltage of the power supply which is now a fixed value, this is not the case in the first solution were the voltage of the DC source was set in accordance to the supercapacitor bank.

The connection between the TF coils and the supercapacitor bank is carried out using the same converter used in the supercapacitor power supply with additional DC source (first solution). Now the DC source is replaced with the existing 12-pulse rectifier. This system was implemented in Simulink and the corresponding circuit can be divided into two parts: the modified power supply and the connection between the elements of the circuit including the power converter. Starting with the 12-pulse rectifier, all the three-phase rectifiers are now connected in series, this is achieved by connecting the output of each rectifier system to the neutral of the secondary three-phase winding linked with the subsequent three-phase rectifier. The neutral points of the windings are located on the power transformers. Now that the rectifiers are all connected in series (single branch) instead of parallel (four branches) there is no need to control the current of each three-phase rectifier individually. As a result, there is only one PI controller which regulates the output current.

The second part of the circuit includes the connection between the rectifier, the CBs and the TF coils. The schematic of the circuit is represented in Figure 8. The block named 12_Pulse Rectifier is a subsystem containing the entire rectifier power supply.

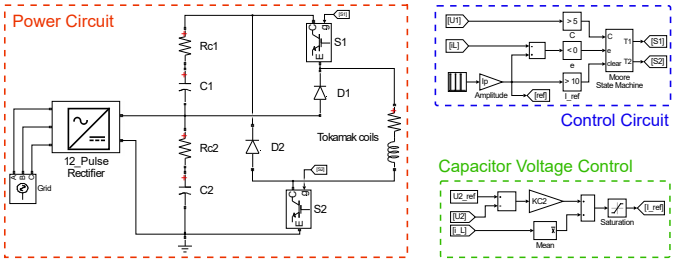

Fig. 8. [Circuit 2] Implementation of the second solution.

This system can be divided into 3 parts: the power circuit, the control circuit and the capacitor voltage control circuit. The power circuit is the main circuit and includes all the major elements and semiconductor power devices. The control circuit (low power) is responsible for providing the control signals to the semiconductor switches (S1 and S2), this part includes the state machine. Finally, a controller for the capacitor voltage is added to the circuit because the supercapacitor bank is in parallel with the rectifier power supply. The purpose of this control system is to correctly charge the supercapacitor bank (C2 and Rc2), therefore, it is responsible for providing the current reference to the PI controller of the rectifier.

Now it will be presented the main results obtained for a pulse of 15000 A with 3 s. The main waveforms are represented in Figure 9, where U1 is the voltage of the ECB, U2 the voltage of the supercapacitor bank, Ip the current reference of the pulse, IL the current flowing through the TF coils, and Irect the current that the rectifier power supply is providing. Figure 9 was obtained for an interval between pulses of 17 s, this value is much smaller than the real rest period, even so it was selected to achieve a clearer figure.

At the beginning of the simulation the ECB is discharged and the supercapacitor bank is charged to approximately 371 V, this value corresponds to almost 99% of the maximum voltage. When the pulse initiates, it takes a little more than 100 ms for the current of the TF coils to reach its reference

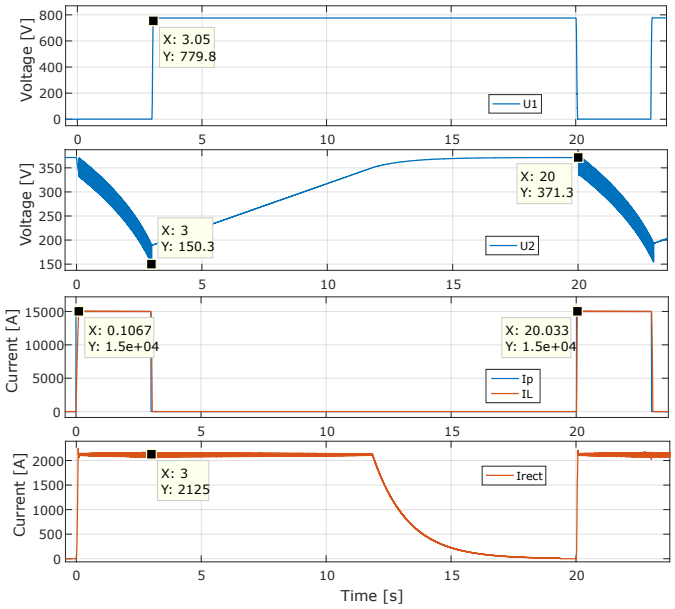

Fig. 9. Operation and main waveforms of the circuit for a pulse of 15000 A with 3 s. Charging and discharging process of the capacitor banks.

(15000 A), the rectifier power supply immediately starts providing current to the coils and the CB. During the pulse the voltage of the supercapacitor bank fluctuates due to the voltage drop on its ESR. The minimum voltage of the supercapacitor bank, reached at the end of the first pulse, is 150.3 V which is enough to sustain the desired current intensity. When the pulse ceases, the ECB charges in 50 ms to approximately 780 V, and remains charged until the beginning of the next pulse. The rectifier power supply keeps feeding current to the supercapacitor bank until its voltage reaches the reference value, near 371 V which is the maximum average voltage of the rectifier. Finally, the ECB is discharged at the beginning of the next pulse which causes the current flowing through the coils to rise much faster, about 33 ms.

C. Energy Recovery Upgrade of the Existing Power Supply (3rd Solution)

In this section, the possibility of adding a supplementary circuit to the 12-pulse rectifier power supply is assessed. The purpose of this complement is to recover the magnetic energy left in the TF coils, avoiding the re-injection of this energy into the public grid. As a result, it is possible to reuse the magnetic energy stored in the coils, on the tokamak, during the next pulse. Also, this solution has the potential to obtain better current rise and fall times. The circuits that will be presented for this solution were developed seeking to achieve the least possible changes on the existing system, while minimizing the number of semiconductors in the active current path to minimize on-state losses. The main configuration of the power supply is not modified, just the connection to the coils.

In order to design a circuit able to recover the energy left in the TF coils it is crucial to size the storage system properly. The capacity of this ESS only needs to be enough to store the remaining magnetic energy. The capacitance of the CB must lead to voltages that minimize the resistive losses of the energy transfer between the coils and the CB. This transfer process happens within time intervals in the order of milliseconds. The first attempt was to use supercapacitors just like before, however this solution is unfeasible because supercapacitors are not capable of fully charging and discharging within periods in the order of milliseconds. However, electrolytic capacitors are capable, this is why they are the selected technology to store the remaining energy on the TF coils. The ECB is sized with a process similar to the one used for the supercapacitor bank.

Regarding the connection between the ECB to the TF coils it is required a circuit based on semiconductor devices, preferably with the minimum number of components needed, specially semiconductors in the active current path. Figure 10 represents the circuit that was implemented. The ECB is represented by the capacitor C1 and the resistor Rc1, which represents the ESR. The thyristor T is used to re-inject the energy stored on the ECB into the coils. The thyristor Td and resistor Rd are used to dissipate the magnetic energy left in the interphase reactors of the rectifier. Adding this branch to the circuit assures that the current flowing through the interphase reactors has a path to flow when the IGBT (S) disconnects the rectifier from the TF coils.

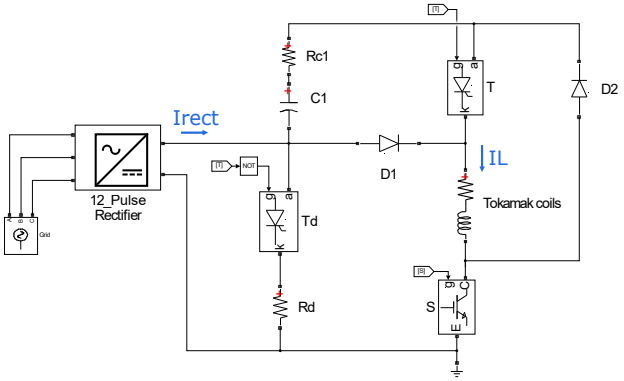

Fig. 10. [Circuit 3.3] Implementation of the recovery circuit.

Now it will be presented the main results obtained for a pulse of 6000 A with 2 s. The current waveforms are represented in Figure 11 (a) and the voltage waveforms in Figure 11 (b). During the pulse, the current at the output of the rectifier (Irect) is the same current flowing through the coils (IL), these two currents are only different at the end of the pulse when the semiconductor devices S and Td switch their operation state. As a result, the current flowing through the coils is redirected to the ECB to recover the magnetic energy left in the coils, and the current coming from the rectifier is redirected to the resistor Rd to dissipate the energy of the interphase reactors. The voltage at the terminals of the ECB (UC) and across the coils (UL) are also represented in Figure 11 (b). It is possible to verify that the CB only charges at the end of the pulse reaching a voltage of 551.1 V which corresponds to approximately 84 % of the energy stored in the TF coils for a pulse of 6000 A. At the beginning of the next pulse the ECB is already charged, therefore, the voltage applied to the coils reaches a peak value of 642 V since the CB discharges in series with the rectifier. As a result, the current rise time is shortened a lot which is shown in Figure 11 (a). The time it takes for the current flowing through the

coils (IL) to reach the reference value (in this case 6000 A) is 97 ms when the ECB is charged and 209 ms when it is discharged. However, this difference is significantly greater if it is considered 96 % of the current reference value instead. When the ECB is charged, it takes approximately 27 ms to reach 96 % of the reference value, this is also the time it takes for the capacitors to discharge. In comparison, when the ECB is discharged it takes 193 ms for the current to reach the same value, which is around 7 times slower. Another benefit of this circuit is the reduction of the over-current at the beginning of the pulse. When the ECB is discharged the peak current is 6403 A, however when it is charged the peak drops to 6071 A.

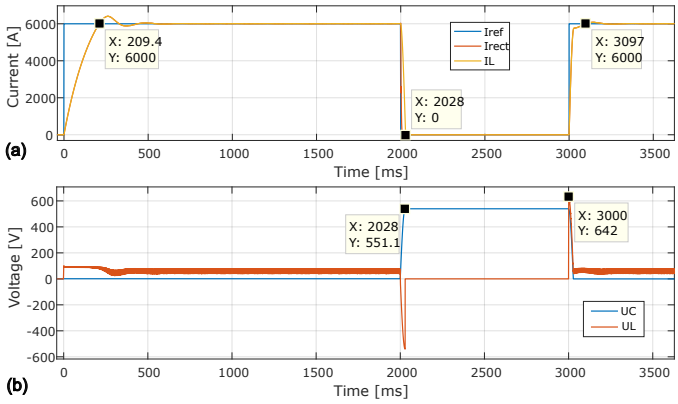

Fig. 11. Waveforms of the circuit for a pulse of 6000 A: (a) main currents; (b) voltage of the ECB and voltage applied to the coils.

V. Discussion and Conclusion

The present paper addresses the preliminary design of an ESS for the fusion reactor named ISTTOK. There are three distinct solutions that stand out, each one having strong advantages but also drawbacks. In this section, these solutions will be compared.

The supercapacitor power supply with an additional DC source was the first option studied. This solution consists of a supercapacitor power supply able to replace the exiting 12-pulse rectifier. This ESS has a supercapacitor bank that charges between the pulses using a relatively low power DC source, and discharges during the pulse. This option is capable of reducing the contracted power tariff since the source of the TF coils becomes the CB instead of the rectifier power supply. Even so, this solution requires many CCs because the CB must provide all the energy needed for the pulse. It is also required a DC power supply to charge the capacitors, as a result, the first option has substantial costs involved.

The modified rectifier power supply with auxiliary capacitor banks was the second option analysed. This solution is a combination between the existing 12-pulse rectifier and a supercapacitor power supply. The configuration of the rectifier is slightly modified in order to obtain a higher output voltage. The power supply feeds the TF coils together with the supercapacitor bank, as a result, this CB does not need to be as large as the one used in the first option. The third solution is adequate if the intention is to increase the maximum intensity of the current supplied to the TF coils.

The energy recovery upgrade of the existing power supply was the third option studied. This solution is an upgrade to the existing rectifier power supply, which consists in an additional circuit that complements the operation of the TF system. The purpose of this upgrade is to store the magnetic energy left in the coils at the end of the pulse in an ECB, so it can be later reused in the tokamak. The efficiency of the recovery process is approximately 84 %. This solution is also capable of avoiding the re-injection of the energy left into the public grid. In this case the CB only stores the magnetic energy remaining in the TF coils which is much less than the energy required for the pulse. Therefore, the number of cells needed in comparison is considerably smaller. This option is the least demanding in terms of components.

Lastly, the solutions and the corresponding circuits that were analysed are illustrated in Table III. This table also shows other circuits that were presented in the thesis but not on the paper. For this paper it was only selected the best circuit for each solution. In summary, the fist solution is the most adequate to reduce the contracted power tariff, the second solution the most appropriate to increase the intensity of the current flowing though the coils, and the third solution the most appropriate to only reuse the energy left in the coils. The most economic option is the circuit 3.1, because it requires less semiconductor devices and capacitor cells. The best solution disregarding the economic aspect is the circuit 1.2, since it is capable of reducing the power demand from the grid, as well as capable of obtaining better waveforms and even able to increase the intensity of current if that is the intention.

References

[1] S. Mirnov, "Tokamak evolution and view to future," *Nuclear Fusion*, vol. 59, Nov. 2018. DOI: 10.1088/1741-4326/aaee92.

[2] V. A. Glukhikh, "Chapter 1 - engineering and physical principles of the magnetic fusion reactor operation," in *Fundamentals of Magnetic Thermonuclear Reactor Design*, 2018, pp. 1–5. DOI: https://doi.org/10.1016/B978-0-08-102470-6.00001-9.

[3] H. R. Mirzaei and R. Amrollahi, "Design, simulation and construction of the taban tokamak," *Plasma Science and Technology*, vol. 20, p. 045 103, Apr. 2018. DOI: 10.1088/2058-6272/aaa669.

[4] H. Fernandes, J. Cabral, C. Varandas, and C. Silva, "20 years of isttok tokamak scientific activity," *Presented at the 24th IAEA Fusion Energy Conference. San Diego, USA*, p. 7, 2012.

[5] J. Santana, V. Anunciada, V. Líbano Monteiro, J. C. Lameira, C. Varandas, H. Fernandes, J. Sousa, and C. Freitas, "One megawatt supply for tokamak isttok," *ELECTRICIDADE, N° 309*, pp. 94–105, Mar. 1995.

[6] M. Aneke and M. Wang, "Energy storage technologies and real life applications – a state of the art review," *Applied Energy*, vol. 179, pp. 350–377, Oct. 2016. DOI: 10.1016/j.apenergy.2016.06.097.

[7] M. Güney and Y. Tepe, "Classification and assessment of energy storage systems," *Renewable and Sustainable Energy Reviews*, vol. 75, Nov. 2016. DOI: 10.1016/j.rser.2016.11.102.

[8] S. Koohi-Fayegh and M. Rosen, "A review of energy storage types, applications and recent developments," *Journal of Energy Storage*, vol. 27, p. 101 047, Feb. 2020. DOI: 10.1016/j.est.2019.101047.

[9] A. Dehghani-sanij, M. Dusseault, E. Tharumalingam, and R. Fraser, "Study of energy storage systems and environmental challenges of batteries," *Renewable and Sustainable Energy Reviews*, vol. 104, pp. 192–208, Apr. 2019. DOI: 10.1016/j.rser.2019.01.023.

[10] M. Khodaparastan and A. Mohamed, "Flywheel vs. supercapacitor as wayside energy storage for electric rail transit systems," *Inventions*, vol. 4, p. 62, Oct. 2019. DOI: 10.3390/inventions4040062.

[11] T. Aljohani, "The flywheel energy storage system: A conceptual study, design, and applications in modern power systems," *International Journal of Electrical Energy*, Jan. 2014. DOI: 10.12720/ijoee.2.2.146-153.

[12] N. Nitta, F. Wu, J. Lee, and G. Yushin, "Li ion battery materials: Present and future," *Materials Today*, vol. 18, Nov. 2014. DOI: 10.1016/j.mattod.2014.10.040.

TABLE III
COMPARISON BETWEEN THE DIFFERENT TOPOLOGIES THAT WERE ANALYSED.

Solution	Circuit	SCB	ECB	IGBTs	Diodes	Thyristors	Extra Elements	Advantages	Drawbacks
1st Supercapacitor Power Supply with Additional DC Source	1.1	Yes	No	2	2	0	Power Supply	Reduces contracted power tariff; Potential to increase maximum current.	Large SCB, requires more cells; Requires new power supply to charge SCB.
	1.2	Yes	Yes	2	2	0	Power Supply	Reduces contracted power tariff; Better current rise and fall times; Potential to increase maximum current.	Large SCB, requires more cells; Requires a new power supply to charge SCB.
2nd Modified Rectifier Power Supply with Auxiliary Capacitor Banks	2	Yes	Yes	2	2	0	Modifications on the rectifier.	Uses the existing rectifier as the SCB charger and assists it during the pulse; Better current rise and fall times; Potential to increase maximum current.	Requires modifications on the existing rectifier power supply.
3rd Energy Recovery Upgrade of the Existing Power Supply	3.1	No	Yes	0	2	1	No	Lowest cost option;	Lowest efficiency of the recovery process.
	3.2	No	Yes	1	2	1	Small CB, Resistor.	Low cost option; Better current rise and fall times.	Requires an additional small CB and a resistor; Slightly affects the waveforms.
	3.3	No	Yes	1	2	1 + 1	Small Thyristor, Resistor.	Low cost option; Better current rise and fall times.	Requires an additional small Thyristor and resistor (inexpensive).

[13] R. Bavithra and B. Abarna, "Performance analysis of electrolytic and film type capacitor," *International Journal of Students' Research in Technology Management*, vol. 3, p. 425, Oct. 2015. DOI: 10.18510/ijsrtm.2015.375.

[14] F. Silva, "Electrónica industrial, fundação calouste gulbenkian," in. 1998.

[15] J. Schnack, S. Bruckner, H. Suncksen, U. Schümann, and R. Mallwitz, "Analysis and optimization of electrolytic capacitor technology for high frequency integrated inverter," *IEEE Transactions on Components, Packaging and Manufacturing Technology*, vol. PP, pp. 1–1, May 2021. DOI: 10.1109/TCPMT.2021.3084371.

[16] F. Silva and S. Pinto, "Control methods for switching power converters," in. Dec. 2007, pp. 935–998, ISBN: 9780080467658. DOI: 10.1016/B978-012088479-7/50052-3.